Research on Chemical Intermediates

Thermal behavior of ammonium octafluorodirhenate(III)

--Manuscript Draft--

Manuscript Number:	RINT-D-22-00172R1
Full Title:	Thermal behavior of ammonium octafluorodirhenate(III)
Article Type:	Original Research
Keywords:	Rhenium; Fluoride; Decomposition; Metal; X-ray diffraction
Corresponding Author:	James Louis-Jean University of Nevada Las Vegas Las Vegas, Nevada UNITED STATES
Corresponding Author Secondary Information:	
Corresponding Author's Institution:	University of Nevada Las Vegas
Corresponding Author's Secondary Institution:	
First Author:	James Louis-Jean
First Author Secondary Information:	
Order of Authors:	James Louis-Jean
	Harry Jang
	Jonathan George
	Frederic Poineau
Order of Authors Secondary Information:	
Funding Information:	National Nuclear Security Administration (DE-NA0003948) — Not applicable
	National Nuclear Security Administration (DE-NA0003180) — Not applicable
Abstract:	The thermal behavior of (NH 4) 2 [Re 2 F 8]•2H 2 O salt was studied in the temperature range 150-700 °C under flowing nitrogen gas. The decomposition products were studied by powder X-ray diffraction (PXRD), scanning electron microscopy (SEM), and energy-dispersive X-ray (EDX) spectroscopy. Results are consistent with the formation of (NH 4) 2 [Re 2 F 8] salt at 150 °C, amorphous rhenium metal at 300 and 400 °C and crystalline rhenium metal at 500 and 700 °C. A mechanism of formation of rhenium metal from (NH 4) 2 [Re 2 F 8]•2H 2 O was proposed. The effect of crystallite size and lattice strain were evaluated at 500 and 700 °C from powder XRD peak broadenings using both Williamson-Hall and the modified Scherrer methods.
Response to Reviewers:	Dear Editorial Board, We are pleased to resubmit for publication the revised version of RINT-D-22-00172 manuscript titled: “Thermal behavior of ammonium octafluorodirhenate(III)”. We thanked the reviewers and editors for their consideration of our work. We appreciated the constructive criticism of the reviewers and the time they took to review the manuscript and below, we addressed their concerns. Reviewer #1: In this work, the thermal decomposition of (NH4)2[Re2F8]*2H2O salt was studied in the temperature range 150-700 °C under flowing nitrogen gas. And a decomposition mechanism of formation of Re metal from (NH4)2[Re2F8]*2H2O was proposed. The results indicated that (NH4)2[Re2F8]*2H2O salt could transform into (NH4)2[Re2F8] at 150 °C, amorphous Re metal at 300-400 °C and crystalline rhenium metal at 500-700 °C. This work is novel and interesting. In my opinion, this manuscript can be accepted

after addressing the following issues:

1. The thermal decomposition of (NH4)2[Re2F8]*2H2O salt can be investigated in the nitrogen gas. How about air atmosphere?

Authors: Under air, the salt is completely volatilized (formation of Re2O7) due to reaction with oxygen in the atmosphere. Therefore, the authors were unable to collect residue materials for any characterization to provide reliable discussion concerning this.

2. In Figure 2, why are the different crystallinity of the products at different decomposition temperatures?

Authors: This is because among other extrinsic factors, the crystallinity of a material typically is induced by temperature.

3. In Figure 3, the content of F element disappears with the increase of temperature. What is F converted to? Please give some data.

Authors: Fluorine atoms disappeared with increasing temperature is indicative to the complete conversion of the salt to metallic rhenium. During the decomposition of the salt, F atoms are expected to be released as HF species. Gas-phase analysis could provide useful data concerning the formation and presence of fluoride species. Unfortunately, the authors do not have access to do this. Nonetheless, equation 1 shows the proposed decomposition mechanism where HF is produced.

4. Reference format needs to be further uniformed.

Authors: The reference list is updated.

Reviewer #2:

- The authors can find details in the attached pdf file. The authors can also find the copyediting marks at the end of pdf file. When the authors revise their manuscript, the authors must send detailed response for the each of referee comments on the manuscript. When the authors revise their manuscript, the authors must highlight the changes you make in the manuscript by using colored text.

Authors: All changes are highlighted in the revised manuscript.

- The authors must supply an ORCID ID for all authors. Getting an ORCID iD is FREE, quick and easy to do through the ORCID registration page: https://orcid.org/register

Authors: James Louis-Jean (https://orcid.org/0000-0002-7711-0967)
Harry Jang (https://orcid.org/0000-0002-1721-4107)
Jonathan George (https://orcid.org/0000-0002-5374-6960)
Frederic Poineau (https://orcid.org/0000-0002-9517-2264)

- The abbreviations should be defined or given full names at their first existences in the main text.

Authors: This is updated in the revised manuscript.

- The authors must use Journal Guide when they are preparing the revised manuscript.

Authors: Yes, the authors used the Guide

- How can we use the obtained data in this research in a physical or application study?

Authors: The manuscript shows promising advantages of producing metallic rhenium with unique controlled morphology and crystallinity. This has potential use where morphology and crystallinity of the metal are critical for various applications (i.e.,

	catalysis). --The authors can monitor these reactions with DTA/TG system. The authors can collect DTA/TG data for the (NH4)2[Re2F8]•2H2O. Therefore, we can obtain more data/details about the decomposition steps. Authors: We have investigated the thermal property of the salt using simultaneous thermal gravimetric analysis (TGA) and differential scanning calorimetry (DSC). Efforts to assign observed thermal events to possible reactions/species could not be predicted reliably. This would best be done using gas-phase analysis, but our laboratory is not equipped with such instrument. Editor's comments: 1. We don't need "the titles" of the cited papers (except for the cited "books".) in our journal in order to save the page spaces. Reference should be re-written according to the format of our journal. Otherwise, I cannot allow the publication of this article. Authors: Yes. The refence list is updated. 2. Please follow our journal's style to modify your revised version since we use only abbreviation of journal names but not full names for references. Please see example in an attached file for your reference. Authors: The reference list is updated.

Thermal behavior of ammonium octafluorodirhenate(III)

James Louis-Jean*, Harry Jang, Jonathan George and Frederic Poineau

Department of Chemistry and Biochemistry, University of Nevada Las Vegas, 4505 S. Maryland Parkway, Las Vegas, Nevada 89154, USA

*Corresponding authors: louisjea@unlv.nevada.edu (JLJ)

Abstract

The thermal behavior of $(NH_4)_2[Re_2F_8]\bullet 2H_2O$ salt was studied in the temperature range 150-700 °C under flowing nitrogen gas. The decomposition products were studied by powder X-ray diffraction (PXRD), scanning electron microscopy (SEM), and energy-dispersive X-ray (EDX) spectroscopy. Results are consistent with the formation of $(NH_4)_2[Re_2F_8]$ salt at 150 °C, amorphous rhenium metal at 300 and 400 °C and crystalline rhenium metal at 500 and 700 °C. A mechanism of formation of rhenium metal from $(NH_4)_2[Re_2F_8]\bullet 2H_2O$ was proposed. The effect of crystallite size and lattice strain were evaluated at 500 and 700 °C from powder XRD peak broadenings using both Williamson-Hall and the modified Scherrer methods.

Keywords: Rhenium; Fluoride; Decomposition; Metal; X-ray diffraction

1. Introduction

The discovery of quadruple metal-metal bond in dirhenate(III) complex (i.e., $[Re_2Cl_8]^{2-}$) led to extensive investigations in the nature of multiple metal-metal bonds and unravel new area of research in catalysis, metal and materials sciences [1–9]. Several complexes containing the $[Re_2X_8]^{2-}$ anions (X = F, Cl, Br, I) have been reported. However, complexes containing the fluoro derivative, $[Re_2F_8]^{2-}$, are relatively rare [10–12]. Only recently a detailed preparation of the ammonium salt, $(NH_4)_2[Re_2F_8]\bullet 2H_2O$ and its reactivity were reported [13–15]. Rhenium complexes containing the $[Re_2X_8]^{2-}$ anion species have been characterized by several techniques [11,12,16–20], including X-ray absorption fine structure (XAFS), single crystal and powder X-ray diffraction, Raman, and theoretical studies. To the best of our knowledge, the thermal behavior of $[Re_2X_8]^{2-}$ salts have not been reported. The thermal analysis behavior could fundamentally provide a further understanding of quadruply bonded metal-metal complexes and the chemistry of rhenium. For example, decomposition products of fluoride salts could be a method to access new binary

fluorides (i.e., ReF_3). In this context, we note that the thermal decomposition of $Ag_2[ReBr_6]$ produced $ReBr_3$ [21].

Our laboratory has been engaged in the chemistry of technetium and rhenium fluorides as well as binary halides [22,23,32–34,24–31]. We prepared $(NH_4)_2[Re_2F_8]•2H_2O$ in the solid state and characterized it in solution by UV-Vis and ^{19}F-NMR and in the solid-state by PXRD and IR spectroscopy; so far no thermal study has been performed on this salt. In this context, we found it necessary to study the thermal behavior of $[Re_2F_8]^{2-}$ salt at high temperatures and investigate the reaction products. In the present work, the thermal behavior of $(NH_4)_2[Re_2F_8]•2H_2O$ under nitrogen atmosphere was investigated in the temperature range 150-700 °C. The decomposition products were analyzed by powder XRD, scanning electron microscope (SEM), and energy dispersive X-ray (EDX). The crystallite size and lattice strain of the decomposition products were evaluated from powder XRD peak broadenings using both Williamson-Hall and the modified Scherrer methods.

2. Experimental

2.1 Materials

All chemicals were purchased from Sigma Aldrich and were used as received without any further purification. Pure nitrogen (N_2) tank was purchased from AirGas, Inc. Thermal decomposition were performed in a Barnstead-Thermolyne 1000 furnace. A schematic representation of the experimental setup is highlighted in reference [35].

Cautions: Due to the corrosive nature of ammonium bifluoride, all chemical manipulations were performed in a well-ventilated fume hood.

2.2 Preparation of $(NH_4)_2[Re_2F_8]•2H_2O$

The $(NH_4)_2[Re_2F_8]•2H_2O$ salt was prepared according to the literature method [13] from the solid-state melt reaction (SSMR) of $(n\text{-}Bu_4N)_2[Re_2Cl_8]$ (497.5 mg, 0.436 mmol) with excess NH_4HF_2 (3.830 mg, 67.14 mmol) at 300 °C for 20 minutes in a box furnace using a loosely capped Teflon beaker. After cooling, the solid violet product was washed with methanol (3 × 4 mL) to remove fluoride impurities and chloride byproducts (**Figure 1**). Then, the hydrated $(NH_4)_2[Re_2F_8]$ salt was extracted by dissolving the solid product in water (2 mL) followed by the addition of

methanol (6 mL) and centrifugation. Lastly, the resulting material was washed with diethyl ether (3 mL) and dried at ambient temperature in aerobic condition. Once completely dried (yield: 240 mg, 92%), the purity of the sample was evaluated using powder X-ray diffraction, which verifies the dark violet material to be single phase (**Figure 1**) with an identical XRD pattern as reported in the literature [13].

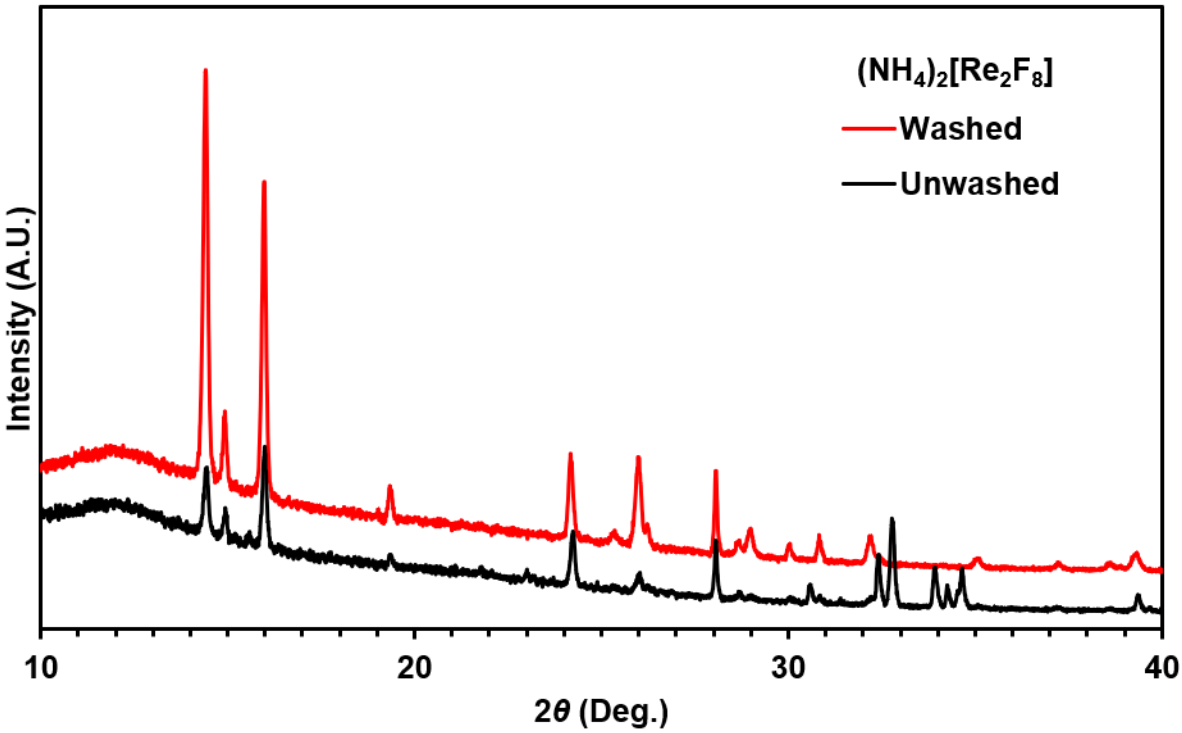

Figure 1. Powder XRD measurements of $(NH_4)_2[Re_2F_8]$ as-synthesized (black trace) and purified (red trace).

2.3 Physical characterizations

Powder X-ray diffraction measurements were collected at ambient temperature on a Bruker D8 advanced diffractometer equipped with Cu-Kα X-rays (λ = 1.5406 Å) and a solid-state Si detector. Samples were pulverized using mortar and pestle before loaded on a low-background Si disk sample holder. Scanning electron microscopy and energy dispersive X-ray spectroscopy analyses were performed using a JEOL model JSM-5610 equipment with secondary-electron. Data

were analyzed using INCA Microanalysis Suite software v4.15 and ImageJ v1.532 software [36]. Simultaneous thermal gravimetric analysis and differential scanning calorimetry measurements were performed in platinum crucible using NETZSCH STA 449 F1 Jupiter instrument operating under argon.

3. Results and discussion

3.1 Thermal decomposition of $(NH_4)_2[Re_2F_8]•2H_2O$

A weighted quantity of $(NH_4)_2[Re_2F_8]•2H_2O$ salt (**Table 1**) was loaded onto an in-house platinum boat constructed with a 4.7 cm × 1.15 cm foil. The Pt boat, supported using a 5-mL alumina boat, was then placed in a quartz tube positioned in the middle of the tube furnace. The right end of the tube was connected to the gas tank (N_2) while the left end was connected to a bubbler. Once the system was purged for 15 minutes, the furnace was programmed (~8 ^oC per minute) and the temperature ramped either to 150, 300, 400, 500 or 700 °C and kept at this temperature for 30 min. Following decomposition, the system was cooled to room temperature under flowing N_2. After reaching room temperature, the sample was weighed (**Table 1**) and analyzed by PXRD (**Figure 2**), TGA and DSC (**Figure *3***), SEM and EDX (**Figure 4**).

Table 1. Mass of $(NH_4)_2[Re_2F_8]•2H_2O$ (mg) prior to reaction and mass (mg) and color of the decomposition products.

$(NH_4)_2[Re_2F_8]•2H_2O$	**Prior reaction (mg)**	**Collected (mg) and color**
150 °C	29.2	27.9 (violet)
300 °C	46.1	30.0 (dark-grey)
400 °C	57.1	36.4 (dark-grey)
500 °C	45.3	27.9 (grey)
700 °C	46.4	29.2 (grey)

Results indicate that at 150 °C, the material is converted to a darker violet color. No significant structural changes were observed in the powder XRD, but the crystallinity of the material was greatly improved (**Figure 2**). Heating to 300 and 400 °C resulted in the formation of dark grey semi-crystalline material. Further treatment at 500 and 700 °C, produced a material with very well-defined X-ray diffraction peaks. The patterns show the presence of pure rhenium metal and match precisely with that of reference number PDF#01-071-6589 without the presence of

impurities. This material is indexed on a hexagonal space group *P63/mmc* with the following lattice parameters a = 2.7611(51) Å, b = 2.7611(51) Å, c = 4.4762(17) Å for the structure at 500 °C and a = 2.7611(25) Å, b = 2.7611(25) Å, c = 4.4858(48) Å for that at 700 °C. We propose that at 500 and 700 °C the $(NH_4)_2[Re_2F_8]\bullet 2H_2O$ salt decomposes to Re metal according to **Eq. 1**.

$$(NH_4)_2[Re_2F_8] \rightarrow 2\ Re_{(s)} + 8\ HF_{(g)} + N_{2(g)} \quad (\mathbf{1})$$

This could occur in a multi-step process starting with the liberation of co-crystallized water molecules followed by the decomposition of the anhydrous salt.

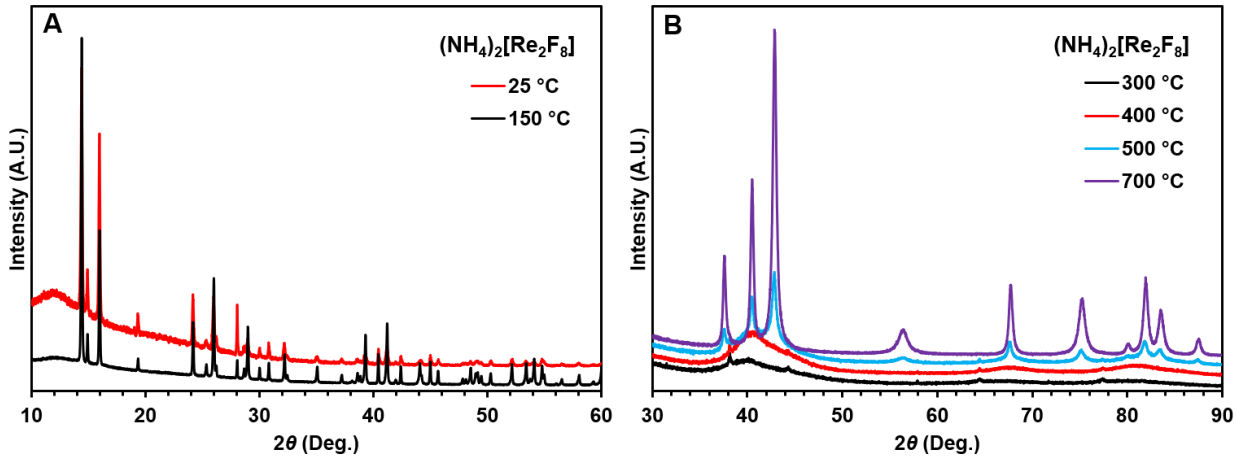

Figure 2. X-ray powder diffraction patterns of $(NH_4)_2[Re_2F_8]\bullet 2H_2O$ salt at 25 and 150 °C (**A**) and the decomposition products at 300, 400, 500 and 700 °C showing the formation of metallic rhenium (**B**).

The thermal decomposition of $(NH_4)_2[Re_2F_8]\bullet 2H_2O$ salt was also monitored using simultaneous TGA/DSC (**Figure *3***). The salt exhibit three distinct endothermic peaks at 129, 205 and 230 °C. The thermal decomposition of the salt follows a complete endothermic process; no exothermic regions are observed from the DSC of the salt. The TGA analysis show the salt is thermally stable up to 150 °C. Above such temperature, the salt exhibits a sharp decrease to 212 °C which is accounted for nearly 42% of the starting material. From 212°C to 245 °C, an additional 14% gradual decrease is observed. Over the temperature range of 245 and 700 °C, a very slow decrease (10%) could be observed. Efforts to assign these thermal events to possible species could not be

predicted reliably. Nonetheless, the collected (34%) material post thermal treatment indicate the presence of metallic rhenium as confirmed by powder XRD.

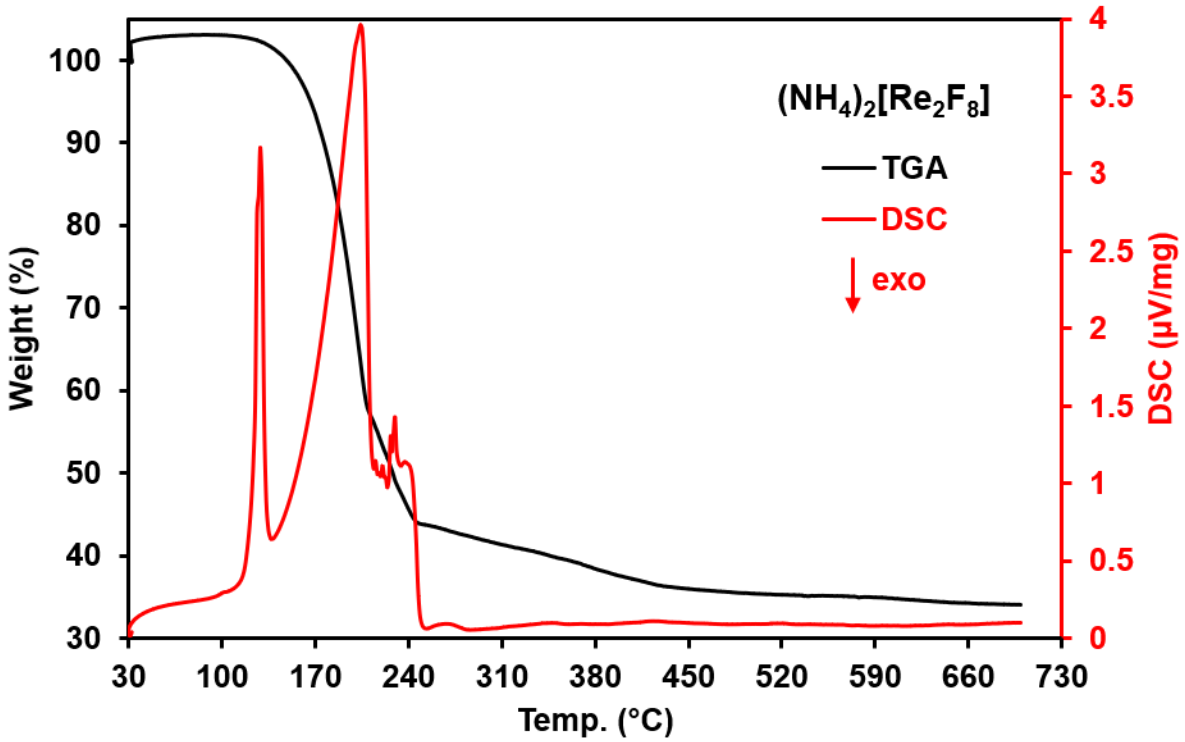

Figure 3. Thermal gravimetric analysis (TGA) and differential scanning calorimetry (DSC) measurements of $(NH_4)_2[Re_2F_8]\bullet 2H_2O$

Given that the broadening of the XRD peaks is due the combined effect of crystallite size and lattice strain, these parameters can be evaluated using the full width at half-maximum (FWHM) of all XRD peaks. This could be achieved through the application of the modified Scherrer method (D-S) and the Williamson-Hall method (W-H) giving λ is the wavelength of the incident X-ray source (0.15406 nm) and k is the shape factor (0.9) [37]. The Scherrer's formula is: $D = k\lambda/\beta \cos\theta$ where D is the crystallite size, β is the FWHM, and θ is the Bragg's diffraction angle. This method does not include the effect of lattice strain in powder XRD peak broadening. For strain induced broadening, the W-H method is applied and is giving as: $\beta \cos\theta = \varepsilon\ 4 \sin\theta + k\lambda/D$. From this expression, ε and kλ/D, respectively, represents the slope and y-intercept, which are extracted from the linear fit of the scattered data of $4 \sin\theta$ versus $\beta \cos\theta$. From this, the crystallite size and lattice strain are calculated [35,38,39]. Giving the poor crystallinity of the

decomposition products at 300 and 400 °C, their XRD patterns were not considered for calculation. Only of the samples treated at 500 and 700 °C were used for calculation. The crystallite size of rhenium metal (**Table 2**) obtained at 700 °C is consistent and in very good agreement using both D-S (174.61 nm) and W-H (175.41 nm) methods. For the sample obtained at 500 °C, major difference is observed between the crystallite size calculated using both methods. Such discrepancy can be the result of lattice imperfections and defects, which affect the crystallinity of the material.

Table 2. Crystallite size (nm) and lattice strain calculated using Debye-Scherrer (D-S) and Williamson-Hall (W-H) methods.

Sample temperature	D-S	W-H
500 °C	95.63	56.07 (4.19×10^{-3})
700 °C	174.61	175.41 (3.92×10^{-4})

SEM images clearly show morphological differences in the $(NH_4)_2[Re_2F_8]\bullet 2H_2O$ salt, before and post thermal treatment (**Figure 4**). At room temperature, a mixture of particles could be observed. This consists primarily of elongated rod-shaped as well as pseudo cubic plate single crystals. The morphology of these particles was drastically changed at 150 °C, which is believed to be a result of dehydration based on weight difference (**Table 1**). Further heating to 300, 400, 500, and 700 °C lead to disappearance of the fluorine peak (0.677 keV) and the presence of only Re peaks (1.842 and 8.651 keV) on the EDX spectra of the decomposition products. This result is consistent with the complete decomposition of $(NH_4)_2[Re_2F_8]\bullet 2H_2O$ according to **Eq. 1** and the formation of Re metal at those temperatures. All EDX spectra were taken on large area and counted for 2-5 minutes.

At 300 °C the formation of amorphous rhenium with rod-like shape and short cylindrical morphologies are observed whereas at 500 °C primarily long needle-like crystals and several elongated cylindrical shaped crystals are detected for polycrystalline rhenium. At 700 °C, this material is almost completely converted to fiber-like shaped crystal of metallic rhenium. The

morphology of these particles is in contrast with other studies resulted in porous rhenium metal, which are driven by liberation of gaseous species at high temperatures [35,40]. Based on this results, the yield (%) of the formation of rhenium metal at 300, 400, 500 and 700 °C from $(NH_4)_2[Re_2F_8]•2H_2O$ decomposition could be, respectively, calculated: 97.9, 95.9, 92.7 and 94.7%.

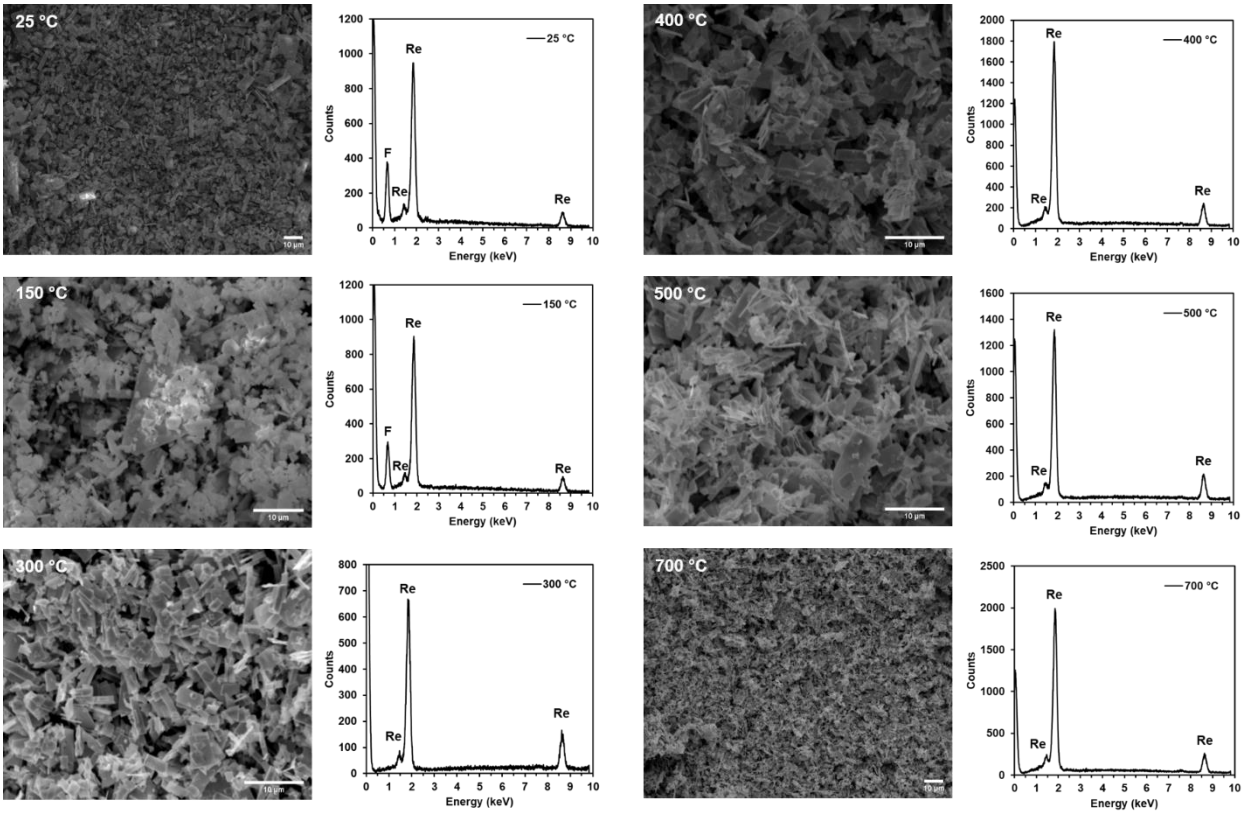

Figure 4. SEM micrograph images and EDX spectrum of the $(NH_4)_2[Re_2F_8]•2H_2O$ salt at 25 °C and the decomposition products at 150, 300, 400, 500 and 700 °C.

Rhenium metal is used in various technological fields [41–43] primarily due to its high melting point and corrosion properties. Given the scarcity of this refractory metal in nature and its high demand, efforts to recycle and reclaim the metal from used materials provide a critical area for research. Currently, several methods are reported for laboratory scale production [43–45] from which the metal could be obtained from the reduction of perrhenate in hydrogen atmosphere. In

addition to this, a number of rhenium compounds (i.e., $C_6H_6N_3[ReO_4]$; $(NH_4)_2[ReX_6]$ X = F, Cl, Br, I) could be converted to rhenium metal in non-reactive environment (i.e., Ar, N_2) [35,46]. This is now expanded to $(NH_4)_2[Re_2F_8]\bullet 2H_2O$, as this study shows its conversion to pure metallic rhenium in very high yield.

4. Conclusion

In summary, the thermal decomposition of $(NH_4)_2[Re_2F_8]\bullet 2H_2O$ has been studied in the temperature range 150-700 °C under flowing nitrogen. The phase purity, chemical composition and morphology of the decomposition product was investigated by powder XRD, SEM and EDX. The diffraction and microscopic results are consistent with the presence of amorphous Re metal (300-400 °C) and crystalline rhenium metal (500-700 °C). This conversion to a highly crystalline metal is driven by temperature. XRD peak broadening, as investigated using both Williamson-Hall and the modified Scherrer method, provides an insight into the structural defect and imperfection of metallic rhenium obtained at 500 °C while at 700 °C those methods show the particle size of rhenium metal to be 174.61 and 175.41 nm, respectively. This study shows that binary fluorides were not obtained from $(NH_4)_2[Re_2F_8]\bullet 2H_2O$ decomposition. In order to further investigate the formation of rhenium binary fluorides, we plan to investigate the thermal decomposition of potassium fluoride salts. In this context, we note that both $K_2[ReF_6]$ and $K_2[Re_2F_8]\bullet 2H_2O$ has been prepared, but their thermal behavior are still unknown. Current works on the thermal behavior of these salts are in progress and results will be reported.

Acknowledgements

This material is based upon work performed under the auspices of the Consortium on Nuclear Security Technologies (CONNECT) supported by the Department of Energy/National Nuclear Security Administration under Award Number DE-NA0003948. In addition, part of this material is based upon work supported by the Department of Energy National Nuclear Security Administration through the Nuclear Science and Security Consortium under Award Number DE-NA0003180.

References

1. F. A. Cotton, N. F. Curtis, C. B. Harris, B. F. G. Johnson, S. J. Lippard, J. T. Mague, W. R.

Robinson, and J. S. Wood, Science (80-.). **145**, 1305 (1964).

2. F. A. Cotton, N. F. Curtis, B. F. G. Johnson, and W. R. Robinson, Inorg. Chem. **4**, 326 (1965).

3. F. a. Cotton and C. B. Harris, Inorg. Chem. **4**, 330 (1965).

4. F. A. Cotton, P. E. Fanwick, and P. A. McArdle, Inorg. Chim. Acta **35**, 289 (1979).

5. B. P. Burton-Pye, F. Poineau, J. Bertoia, K. R. Czerwinski, L. C. Francesconi, and A. P. Sattelberger, Inorg. Chim. Acta **453**, 724 (2016).

6. R. J. H. Clark and M. J. Stead, Inorg. Chem. **22**, 1214 (1983).

7. F. Poineau, A. P. Sattelberger, E. Lu, and S. T. Liddle, in *Mol. Met. Bond. Compd. Synth. Prop.* (Wiley Blackwell, 2015), pp. 175–224.

8. F. Poineau, P. M. Forster, T. K. Todorova, E. V. Johnstone, W. M. Kerlin, L. Gagliardi, K. R. Czerwinski, and A. P. Sattelberger, Eur. J. Inorg. Chem. **2014**, 4484 (2014).

9. F. Poineau, E. V. Johnstone, P. M. Forster, L. Ma, A. P. Sattelberger, and K. R. Czerwinski, Inorg. Chem. **51**, 9563 (2012).

10. G. Henkel, G. Peters, W. Preetz, and J. Skowronek, Zeitschrift Für Naturforsch. B **45**, 469 (1990).

11. S. D. Conradson, A. P. Sattelberger, and W. H. Woodruff, J. Am. Chem. Soc. **110**, 1309 (1988).

12. D. E. Morris, C. D. Tait, R. B. Dyer, J. R. Schoonover, M. D. Hopkins, A. P. Sattelberger, and W. H. Woodruff, Inorg. Chem. **29**, 3447 (1990).

13. S. Mariappan Balasekaran, T. K. Todorova, C. T. Pham, T. Hartmann, U. Abram, A. P. Sattelberger, and F. Poineau, Inorg. Chem. **55**, 5417 (2016).

14. S. M. Balasekaran, A. P. Sattelberger, B. Noll, A. Hagenbach, and F. Poineau, Zeitschrift Für Anorg. Und Allg. Chemie **645**, 27 (2019).

15. S. M. Balasekaran, A. P. Sattelberger, A. Hagenbach, and F. Poineau, Inorg. Chem. **57**, 319 (2018).

16. F. Poineau, L. Gagliardi, P. M. Forster, A. P. Sattelberger, and K. R. Czerwinski, Dalt. Trans. 5954 (2009).

17. F. A. Cotton, B. A. Frenz, B. R. Stults, and T. R. Webb, J. Am. Chem. Soc. **98**, 2768 (1976).

18. L. Gagliardi and B. O. Roos, Inorg. Chem. **42**, 1599 (2003).

19. X.-B. Wang and L.-S. Wang, J. Am. Chem. Soc. **122**, 2096 (2000).

20. J. Beck and G. Zink, J. Chem. Crystallogr. **41**, 1185 (2011).

21. F. A. Cotton, S. J. Lippard, and J. T. Mague, Inorg. Chem. **4**, 508 (1965).
22. F. Poineau, J. Louis-Jean, H. Jang, C. Higgins, Samundeeswari, M. Balasekaran, D. Hatchett, and A. P. Sattelberger, SN Appl. Sci. **1**, (2019).
23. J. Louis-Jean, S. M. Balasekaran, A. Hagenbach, and F. Poineau, Acta Cryst. E **75**, 1158 (2019).
24. J. Louis-Jean, S. M. Balasekaran, D. Smith, A. Salamat, C. T. Pham, and F. Poineau, Acta Cryst. E **74**, 646 (2018).
25. J. Louis-Jean, P. M. Forster, S. M. Balasekaran, C. T. Pham, and F. Poineau, J. Fluor. Chem. **252**, (2021).
26. S. M. Balasekaran, A. Hagenbach, and F. Poineau, Inorg. Chem. Commun. **119**, 108064 (2020).
27. S. Mariappan Balasekaran, K. Lawler, A. Hagenbach, A. Abram, U. Abram, A. Sattelberger, and F. Poineau, Eur. J. Inorg. Chem. **2**, 4129 (2019).
28. F. Poineau, E. E. Rodriguez, P. M. Forster, A. P. Sattelberger, A. K. Cheetham, and K. R. Czerwinski, J. Am. Chem. Soc. **131**, 910 (2009).
29. F. Poineau, E. V Johnstone, P. F. Weck, P. M. Forster, E. Kim, K. R. Czerwinski, and A. P. Sattelberger, Inorg. Chem. **51**, 4915 (2012).
30. F. Poineau, C. D. Malliakas, P. F. Weck, B. L. Scott, E. V. Johnstone, P. M. Forster, E. Kim, M. G. Kanatzidis, K. R. Czerwinski, and A. P. Sattelberger, J. Am. Chem. Soc. **133**, 8814 (2011).
31. F. Poineau, E. V. Johnstone, P. F. Weck, E. Kim, P. M. Forster, B. L. Scott, A. P. Sattelberger, and K. R. Czerwinski, J. Am. Chem. Soc. **132**, 15864 (2010).
32. E. V. Johnstone, F. Poineau, P. M. Forster, L. Ma, T. Hartmann, A. Cornelius, D. Antonio, A. P. Sattelberger, and K. R. Czerwinski, Inorg. Chem. **51**, 8462 (2012).
33. P. F. Weck, E. Kim, F. Poineau, E. E. Rodriguez, A. P. Sattelberger, and K. R. Czerwinski, Inorg. Chem. **48**, 6555 (2009).
34. F. Poineau, E. V Johnstone, K. R. Czerwinski, and A. P. Sattelberger, Acc. Chem. Res. **47**, 624 (2014).
35. J. Louis-Jean, H. Jang, A. J. Swift, and F. Poineau, ACS Omega **6**, 26672 (2021).
36. C. A. Schneider, W. S. Rasband, and K. W. Eliceiri, Nat. Methods **9**, 671 (2012).
37. J. I. Langford and A. J. C. Wilson, J. Appl. Cryst. **11**, 102 (1978).

38. M. Ahmadipour, M. J. Abu, M. F. Ab Rahman, M. F. Ain, and Z. A. Ahmad, Micro Nano Lett. **11**, 147 (2016).

39. A. Khorsand Zak, W. H. Abd. Majid, M. E. Abrishami, and R. Yousefi, Solid State Sci. **13**, 251 (2011).

40. S. Sharif Javaherian, H. Aghajani, and H. Tavakoli, Miner. Process. Extr. Metall. **127**, 182 (2018).

41. J. Louis-Jean, J. D. Inglis, S. Hanson, A. Pollington, D. Meininger, S. Reilly, and R. Steiner, J. Radioanal. Nucl. Chem. (2021).

42. J. C. Carlen and B. D. Bryskin, Mater. Manuf. Process. **9**, 1087 (1994).

43. U. Kesieme, A. Chrysanthou, and M. Catulli, Int. J. Refract. Met. Hard Mater. **82**, 150 (2019).

44. O. G. Kuznetsova, A. M. Levin, M. A. Sevostyanov, and A. O. Bolshih, J. Phys. Conf. Ser. **1134**, 012032 (2018).

45. R. P. Singh Gaur, T. A. Wolfe, and S. A. Braymiller, Int. J. Refract. Met. Hard Mater. **50**, 79 (2015).

46. J. Louis-Jean, A. J. Swift, D. W. Hatchett, and F. Poineau, Inorg. Chem. Commun. **140**, 109482 (2022).